Journal of ELECTRONIC MATERIALS, Vol. 47, No. 11, 2018
https://doi.org/10.1007/s11664-018-6608-8

Effect of Complexing Agents on Properties of Electrodeposited InSb Thin Films

JOGINDER SINGH[1] and RAJARAM POOLLA[1,2]

1.—School of Studies in Physics, Jiwaji University, Gwalior, MP 474011, India. 2.—e-mail: prajaram@ymail.com

InSb thin films have been prepared by a one-step electrodeposition technique using sodium tartrate, sodium citrate, and ethylenediamine tetraacetic acid (EDTA) as complexing agents in addition to citric acid. The growth and properties of the InSb thin films were investigated by x-ray diffraction (XRD) analysis, scanning electron microscopy (SEM), energy-dispersive analysis of x-rays (EDAX), and Raman spectroscopy to study the effects of the complexing agents. All samples were annealed in vacuum at 300°C for 1 h prior to characterization. XRD analysis along with Raman spectroscopy revealed that good-quality InSb thin films with zincblende structure were obtained when using sodium citrate and sodium tartrate as complexing agents. EDAX showed that the elemental composition of the films could be controlled by varying the concentrations of complexing agents. Films having the best stoichiometry were obtained when using either 0.2 M sodium citrate or 0.2 M sodium tartrate. Scanning electron microscopy (SEM) showed that the stoichiometric films synthesized using sodium citrate were uniformly covered with submicron-sized particles of spherical shape.

Key words: InSb, electrodeposition, thin films, XRD, Raman spectra, SEM

INTRODUCTION

Due to their excellent properties, III–V semiconductors (AlSb, GaSb, InSb, GaAs, etc.) have been used in many applications in the field of novel optoelectronic and nanoelectronic devices. Among these various candidates, indium antimonide (InSb) is a direct-bandgap semiconductor with low energy bandgap of 0.17 eV at 300 K and 0.23 eV at 80 K, corresponding to an infrared (IR) cutoff wavelength of 6.2 μm at 300 K.[1,2] It is one of the most studied binary III–V semiconductors, possessing many excellent properties such as high electron mobility (8×10^4 cm^2 V^{-1} s^{-1}) and hole mobility (1250 cm^2 V^{-1} s^{-1}), large spin–orbit coupling (Δ = 0.80 eV) and large Landé g-factor.[3–5] InSb is an excellent material for use in the field of infrared detectors and filters operating in the spectral range of 3 μm to 5 μm, owing to its low energy bandgap, large dielectric constant, and high electron mobility.[6,7] It is also known to be a promising material for fabrication of high-speed and low-power logic transistors,[8,9] gas sensors,[10] magnetoresistive sensors,[11–13] speed-sensitive sensors,[14,15] and thermoelectric generators.[16,17]

InSb thin films have been grown by different techniques such as radiofrequency sputtering,[18] solid-source molecular beam epitaxy,[19,20] metalorganic chemical vapor deposition (MOCVD),[21,22] and vacuum evaporation.[23] Among the nonvacuum techniques, electrodeposition is simple and attractive because of its simplicity, requirement for only low-cost source materials, large-area deposition, inexpensive equipment, and room-temperature growth, compared with other methods.[24,25] In addition, unlike chemical gas-phase methods, poisonous gaseous precursors are not required.[26] The technique is useful for synthesis of compound semiconductors such as InSb, where the large vapor pressure difference between In and Sb may result in nonstoichiometric growth at high temperature.[27,28] The

(Received February 15, 2018; accepted August 14, 2018; published online August 25, 2018)

technique depends on deposition parameters such as the reduction potential, current density, concentration of metal ions in the bath, and pH of the electrolyte solution. The only major disadvantage of this technique is that the substrate must be conducting. However, without use of a suitable complexing agent, electrodeposition of InSb thin films from an aqueous bath is difficult, because of the large difference in reduction potential between In (– 0.340 V) and Sb (+ 0.212 V).[29] To bring the reduction potentials of the two elements closer to one another, it is essential to add a complexing agent to the electrochemical bath. Furthermore, such addition of a complexing agent to the electrolytic bath is found to improve the quality of the thin film electrodeposited on the substrate, including its uniformity, adhesion, and crystallinity.[30,31] Several researchers have reported electrodeposition of InSb, mainly from aqueous solutions containing citric acid plus sodium citrate as complexing agent. In all work reported to date, InSb was electrodeposited using fixed concentration of sodium citrate. Machesney et al. electrodeposited InSb thin films on Ti, indium-doped tin oxide (ITO), and Cu substrates; all the films contained either In or Sb along with InSb, and the stoichiometry varied with the potential for Ti but, for ITO and Cu, was mostly independent of the reduction potential.[32] Fulop et al. reported growth of binary compound InSb onto polycrystalline Cu and single-crystal Si substrates, achieving thicknesses in the micron range. The stoichiometry was found to depend primarily on the ratio of $InCl_3$ to $SbCl_3$ in the electrolyte, but to be less dependent on the applied potential and pH.[33] Khan et al.[34,35] fabricated nanowire arrays and observed very high photoconduction response to IR radiation, demonstrating their potential for use in IR detector applications. Hnida et al.,[36] Singh et al.,[37] and Das et al.[38] also reported growth of InSb nanowires using electrodeposition. Hsieh et al.[39] and Yang et al.[40] synthesized stoichiometric InSb thin films using ionic liquid 1-butyl-1-methylpyrrolidinium dicyanamide (BMP-DCA) and water-stable 1-ethyl-3-methylimidazo chloride/tetrafluoroborate ionic liquid, respectively.

In an earlier paper, the authors reported electrodeposition of InSb using a fixed concentration of sodium citrate.[41] This work presents a comparison of the structural, morphological, compositional, and optical properties of InSb thin films electrodeposited using three different complexing agents, viz. sodium citrate, sodium tartrate, and ethylenediamine tetraacetic acid. The effect of varying the concentration of sodium citrate on the growth and properties of the InSb thin films is also presented. The motivation for this work is that electrodeposited InSb could find applications in low-cost infrared detectors, gas sensors, etc.

EXPERIMENTAL PROCEDURES

Materials

Sodium citrate ($Na_3C_6H_5O_7{\cdot}2H_2O$), sodium tartrate ($Na_2C_4H_4O_6$), ethylenediamine tetraacetic acid ($C_{10}H_{16}O_8N$), and citric acid ($C_6H_8O_7{\cdot}H_2O$) were obtained from Fisher Scientific, India; Indium chloride ($InCl_3$) and antimony chloride ($SbCl_3$) were obtained from CDH, India. All chemicals were of analytical reagent (AR) grade and were used as received without further purification. Deionized water (H_2O) was used as the main solvent.

Synthesis

An EG&G PARC (VERSASTAT-II) computer-controlled potentiostat was used for cyclic voltammetry (CV) studies and the electrodeposition process. In this work, the electrolyte used in the electrochemical bath was an aqueous solution of 0.05 M indium trichloride ($InCl_3$), 0.04 M antimony trichloride ($SbCl_3$), 0.30 M citric acid ($C_6H_8O_7{\cdot}H_2O$), and different additional complexing agents, viz. sodium citrate ($Na_3C_6H_5O_7{\cdot}2H_2O$), sodium tartrate ($Na_2C_4H_4O_6$), or ethylenediamine tetraacetic acid ($C_{10}H_{16}O_8N$). All solutions were prepared in double-deionized water. Citric acid was used to dissolve antimony trichloride, as otherwise it precipitates from water; the acid also helps maintain the pH (around 3.0) in the bath. Thin films were grown from various electrolytic baths, all having the same quantity of citric acid. Although citric acid itself is a complexing agent, additional complexing agents were required to produce stoichiometric InSb films. In this work, only the other additives (e.g., sodium citrate and sodium tartrate) are called complexing agents while citric acid is, for the most part, not treated as one. In general, the concentrations of the additional complexation agents were fixed at 0.2 M, but the effect of varying the concentration on the film properties is also presented, for sodium citrate.

A three-electrode system with graphite rod as counterelectrode, Ag/AgCl as reference electrode, and copper sheet substrate as working electrode was used for this study. The copper sheets were cleaned ultrasonically in distilled water and acetone, then rinsed in distilled water again. All thin films were grown at room temperature at a potential of – 1.3 V versus Ag/AgCl. Each film was electrodeposited for a duration of 15 min, then annealed at 300°C in vacuum for 1 h. The range of potentials suitable for codeposition of In and Sb, for electrolytes containing different complexing agents, was obtained using cyclic voltammetry. For this purpose, CV studies were performed on individual solutions containing indium and antimony and mixtures of In and Sb. The cyclic voltammograms were recorded from 1.0 V to – 1.5 V at scan rate of 20 mV/s.

The crystallographic phase of the films was investigated using a Philips D8 Advance x-ray diffractometer with Cu K_α radiation at a wavelength of 1.5406 Å. Surface morphology and compositional studies were carried out using a Philips FE-SEM/EDAX (Quanta 200 FEG) microscope equipped with an energy-dispersive analysis of x-rays (EDAX) analyzer. Raman studies were carried out on the samples using a confocal Raman spectrometer. Optical measurements were performed using a PerkinElmer Spectrum RX-IFTIR spectrophotometer (scan range 4000 cm^{-1} to 250 cm^{-1}).

RESULTS AND DISCUSSION

Electrochemistry of In and Sb

To understand why the deposition potentials of In and Sb can be brought together, consider the electrochemical reactions of indium and antimony ions.[42,43]

$$In^{3+} + 3e^- \leftrightarrow In(s) \quad (1)$$

In the above reduction reaction, which occurs at the cathode, the electrode potential E is related to the standard reduction potential (or equilibrium potential) E^0 by the Nernst equation,

$$E_{In} = E^0_{In} + \frac{RT}{3F}\ln\left(\frac{a_{In^{3+}}}{a_{In}}\right) \text{ or } E = -0.338V + 0.0197\log\frac{a_{In^{3+}}}{a_{In}}. \quad (2)$$

Similarly, for Sb we can write

$$SbCl_3 \xrightarrow{H_2O} SbO^+ + 2H^+ + 3Cl^- \quad (3)$$

The actual electrochemical reaction can be written as

$$SbO^+ + 2H^+ + 3e^- \leftrightarrow Sb(s) + H_2O \quad (4)$$

The Nernst equation for the reduction of Sb ions is

$$E_{Sb} = E^0_{Sb} + \frac{RT}{3F}\ln\left(\frac{a_{SbO^+}}{a_{Sb}}\right) + \frac{2RT}{3F}\log a_{H^+}, \quad (5)$$

or

$$E_{Sb} = +0.205V + 0.0197\log\frac{a_{SbO^+}}{a_{Sb}} - 0.0393pH, \quad (6)$$

where $a_{In^{3+}}$ and a_{SbO^+} are the activities of the ions in solution, a_{In} and a_{Sb} are the activities of the atoms in the solid deposit, F is the Faraday constant, E^0 is the standard electrode potential of each constituent with respect to the normal hydrogen electrode, and R is the ideal gas constant. In(s) and Sb(s) are the quasisolid forms of In and Sb at the cathode in the deposition. For stoichiometric codeposition, the reduction potentials of the two ions must be close to each other. However, the standard potentials for In and Sb are − 0.33 V and + 0.20 V, respectively, differing by as much as 0.53 V. Equations 2 and 6 suggest that the shift in potentials E is determined by the activities $a_{In^{3+}}$, a_{In}, a_{Sb}, and a_{SbO^+}. The activity of a given species, which is a measure of its reaction rate, is closely related to the concentration of the species in the electrolyte, and can be written as $a_{In} = \gamma_{In} \times [In]$ and $a_{Sb} = \gamma_{Sb} \times [Sb]$ and so on, where γ is the activity coefficient and the quantity in square brackets is the concentration in the electrolyte. The reduction potential of metals can thus be brought close to each other by reducing the concentration of Sb ions and/or increasing the In ion concentration. However, this would require a drastic reduction in the concentration of $SbCl_3$ in the bath, which is not practical. Another option is use of a suitable additive such as a complexing agent, which can selectively reduce the activity coefficient of Sb ions, thus leading to a shift in the electrode potential to negative values. For InSb compound formation, sodium citrate and sodium tartrate seem to be suitable complexing agents that, when added to the electrolytic bath, could cause the reduction potential of the noble metal Sb to be shifted towards negative voltages. Sodium citrate and sodium tartrate make strong complexes with Sb through binding of Sb ions with citrate or tartrate ions, thus reducing the activity and shifting the reduction potential of Sb ions to negative voltages. In contrast, indium ions are not greatly affected by citrate or tartrate ions (at least at low concentrations of the additives), forming probably only weak complexes, not causing a major shift in the In electrode potential. Thus, addition of sodium citrate or sodium tartrate shifts the Sb electrode potential from positive to negative values, thus bringing it closer to that of In, which is at negative potential anyway.

Cyclic Voltammetry

Cathodic electrodeposition of InSb is based on coreduction of Sb^{3+}/Sb and In^{3+}/In. The electrochemical behavior of the electrolytes containing In and Sb salts dissolved in water plus citric acid, with and without additional complexing agents, was analyzed using cyclic voltammetry. All the potentials given here were measured with respect to the Ag/AgCl reference electrode. The cyclic voltammograms (CV) are shown in Fig. 1; Curve (a) shows the CV for the electrolyte in the absence of any complexing agent (except for citric acid). The forward scan in the cathodic direction shows mainly two waves, one at around − 0.690 V and another at around − 1.0 V versus Ag/AgCl, corresponding to reduction of Sb and In, respectively. It can be seen that the two main waves are not very obvious in Fig. 1a. The height of the current wave of each species is proportional to the concentration of the species, among other parameters; for example, in the case of indium, the current wave is related to the indium ion concentration $[In^{3+}]$ in the following way: $I_{wave} \propto 3F[In^{3+}]$; and since the concentrations of the In and Sb salts were only 0.05 M ($InCl_3$) and

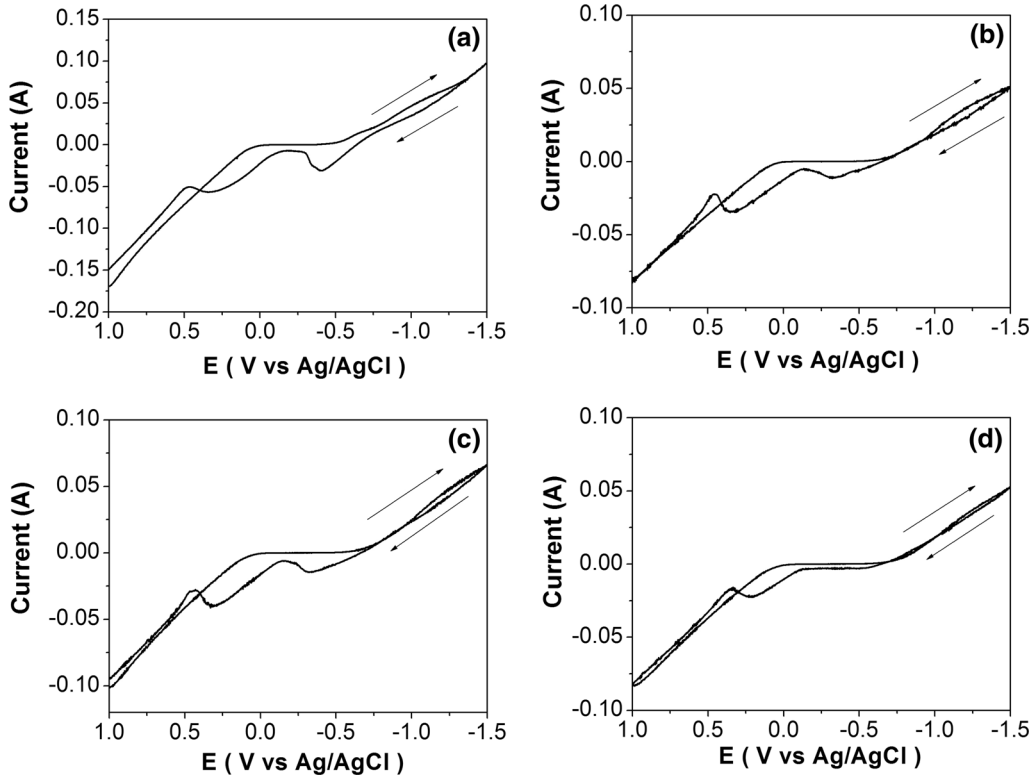

Fig. 1. Cyclic voltammograms of InSb thin films grown from baths containing 0.05 M $InCl_3$, 0.04 M $SbCl_3$, and 0.30 M citric acid with (a) no additional complexing agent, (b) 0.20 M sodium citrate, (c) 0.20 M sodium tartrate, and (d) 0.20 M EDTA.

0.04 M ($SbCl_3$), for the scale of the current plotted, the waves were not very prominent. A sharp anodic peak at − 0.4 V belonging to indium and a broader hump at + 0.340 V for antimony appear in the reverse scan, indicating stripping of indium and antimony from the electrodeposit. InSb films electrodeposited from such a bath are found to have excess indium with only about 30% antimony. Curves (b) and (c) show the CV curves for the InSb electrolytes containing sodium tartrate and sodium citrate, respectively. In the forward scan, the reduction currents of Sb and In are not separately discernible and the current rises below −0.9 V, such as to indicate that the waves of Sb and In have merged together; this suggests that reduction of In and Sb occurred at around the same potential. In the reverse scan, seen in (b) and (c), the anodic current peaks of In are reduced while those of Sb are enhanced in magnitude compared with the corresponding peaks of (a). Addition of sodium citrate and sodium tartrate results in nucleation loops[44,45] in the CV curves, indicating formation of nuclei, i.e., crystallization of products. Such a nucleation loop is not present in curve (a), i.e., the CV curve obtained in the absence of sodium citrate and tartrate. The CV curves are almost identical for both complexing agents, and the films deposited from these baths were found to be stoichiometric, indicating that both sodium citrate and sodium tartrate are suitable for growth of InSb. Figure 1d shows the CV results for the electrolyte containing EDTA as complexing agent. The very small shift in the reduction potential and the presence of a strong anodic peak for antimony and a very weak anodic peak for indium suggest that films deposited from this bath would be antimony rich, as confirmed by EDAX (Table III). It can be seen that the ratio of the Sb to In anodic peaks is larger than unity in Fig. 1b and c, although the films deposited from these baths were stoichiometric according to EDAX. This can be explained by the fact that that some species interact more strongly than others with the electrode on which deposition occurs, leading to irreversible effects. Interactions can lead to reduced stripping from the deposit and thus reduced current, which is perhaps true for indium in this case. Thus, the anodic peaks may not always be directly proportional to the atomic concentrations, although a larger peak can mean a higher concentration.

The effect of one of the complexing agents, viz., sodium citrate, on the growth and properties of the deposit was studied in more detail. To analyze the influence of the concentration of the complexing agent, the quantity of sodium citrate in the electrochemical bath was varied from 0.05 M to 0. 4 M. Figure 2 shows the CV plots for the In–Sb system with different concentrations of sodium citrate. All the CV curves are plotted in the same figure for easy comparison. These curves show that the current density is significantly reduced with increase in the

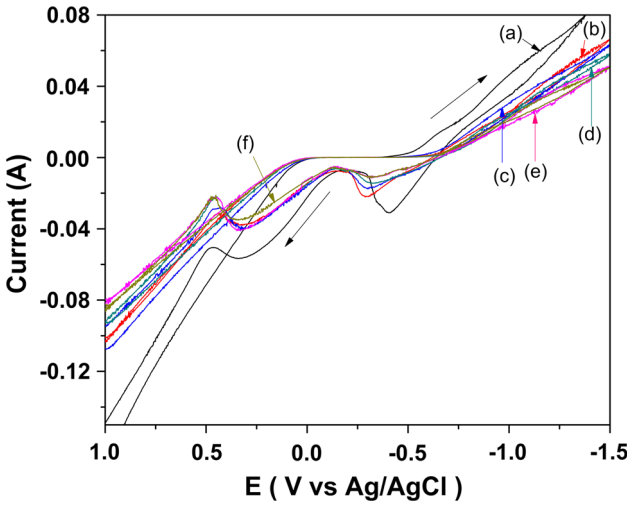

Fig. 2. Cyclic voltammograms of InSb thin films grown from baths containing 0.05 M $InCl_3$, 0.04 M $SbCl_3$, and 0.30 M citric acid with (a) no sodium citrate, (b) 0.05 M sodium citrate, (c) 0.10 M sodium citrate, (d) 0.15 M sodium citrate, (e) 0.20 M sodium citrate, and (f) 0.30 M sodium citrate.

sodium citrate concentration in the electrochemical bath. This effect can be explained by the fact that, with increase in the sodium citrate concentration, the conductivity of the bath decreases. From the CV curves, it can be seen that the intensity of the anodic peaks related to indium gradually decreased as the sodium citrate concentration in the electrolyte was increased from 0.05 M to 0.2 M. As the peak corresponding to In diminishes, the peak corresponding to Sb increases, showing that the quantity of Sb deposited increases. EDAX compositional results (Table IV), discussed below, agree with the CV analysis in that, as the concentration of complexing agent (sodium citrate) in the bath was increased, the indium content reduced while the antimony content increased.

Citric acid, which was primarily used to dissolve $SbCl_3$ and prevent its precipitation from the bath mixture, is known to form a complex with Sb ions, reducing their activity, as already discussed for citrate ions in the previous section. The indium ions are less influenced by citric acid, and the activity of indium remains high. This explains why the deposited films contained more indium than antimony atoms. Although citric acid contributes to bringing the potentials of Sb and In closer, it was used in moderation to avoid a very low-pH bath. Additional complexing agents such as sodium citrate were therefore used. Citrate ions bind strongly with Sb ions to reduce their activity, but In ions form only weak complexes with citrate ions. Therefore, at low and moderate concentrations of citrate ions, the deposition potential of In only undergoes a minor shift whereas that of Sb is shifted by a significant amount, leading to merging of the deposition potentials. However, at relatively high concentrations of sodium citrate, when perhaps the Sb ion complexation has reached its maximum limit, the number of indium ions forming complexes probably rises, making them (indium ions) sluggish with reduced activity. Thus, when the sodium citrate concentration is increased beyond a limit, the Sb potential does not undergo further shift but the indium potential shifts slightly to negative potentials. Therefore, at a given electrode potential, the rate of Sb deposition remains constant, but the rate of In deposition dips as the concentration of citrate ions is increased. This explains why increase of the sodium citrate or sodium tartrate reduces the deposition rate of In relative to that of Sb, leading to near-stoichiometric growth. There are no reports in the literature to support this argument, mainly due perhaps to the fact that similar work has only been reported for relatively low concentrations of sodium citrate. Chraibi et al.[42] used sodium citrate at concentrations up to 25 mM for electrodeposition of $CuInSe_2$. As argued above, at sodium citrate concentrations above 0.15 M, the effects of Sb complexation begin to saturate, and the effects of In complexation become evident. As the citrate ion concentration is further increased, the activity of Sb does not undergo any further change, whereas that of In continues to fall slowly. This can explain the experimentally observed fact that the ratio of Sb to In atoms in the deposit increases slightly with the citrate ion concentration (Table IV) at high citrate ion concentrations.

X-ray Diffraction Studies

Figure 3 shows the XRD patterns of the thin films grown from the electrochemical baths (electrolytes) with and without addition of complexing agents (except for citric acid). All the films were annealed at 300°C in vacuum for 1 h to improve their structural and compositional properties. Annealing the samples is beneficial, provided it is done at the right temperature and for the right duration. Annealing InSb at temperatures above 350°C for 0.5 h or more reportedly leads to deterioration of the surface.[46,47] It may also cause vaporization of low-vapor-point elements such as Sb. InSb itself, with vaporization point of 525°C, begins to evaporate above 500°C.[48] Figure 3a shows the XRD patterns of the films electrodeposited from a bath without addition of any complexing agent. The pattern shows low-intensity peaks for InSb as well as indium, indicating that the films were a mixture of InSb and In. Compositional studies also showed that the films grown without any complexing agent were highly nonstoichiometric, containing excess In.

The diffractograms of InSb thin films electrodeposited from baths containing sodium citrate and sodium tartrate are shown in Fig. 3b and c, respectively. All the XRD patterns exhibit diffraction peaks corresponding to (111), (220), (311), (400), and (331) planes of the zincblende structure in

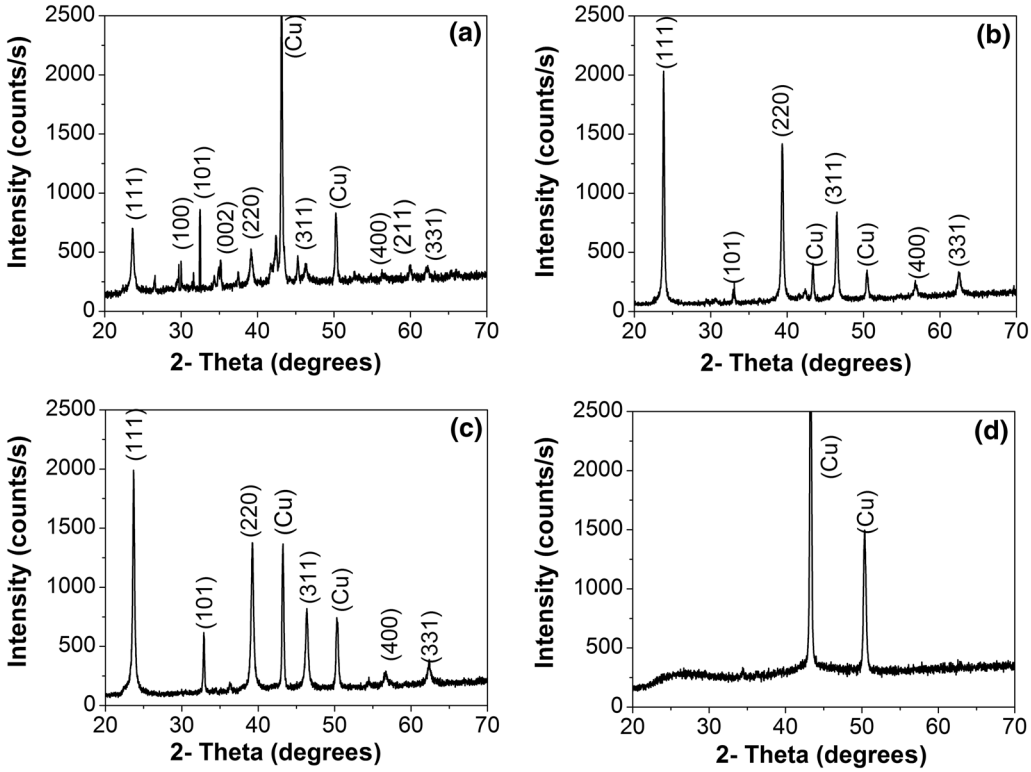

Fig. 3. XRD patterns of InSb thin films grown from baths containing 0.05 M $InCl_3$, 0.04 M $SbCl_3$, and 0.30 M citric acid with (a) no additional complexing agent, (b) 0.20 M sodium citrate, (c) 0.20 M sodium tartrate, and (d) 0.20 M EDTA.

JPPDF data file no. 00-0519-0577. Apart from the above-mentioned crystallographic reflections of InSb, an additional low-intensity peak of In is observed for all the samples. The intensity of this additional (101) peak for elemental indium is slightly stronger when sodium tartrate is used as complexing agent, indicating that, when tartrate was used, most of the crystallites of elemental indium had their (101) planes in the same direction. Films grown from the bath containing EDTA as complexing agent did not exhibit any diffraction peaks for InSb, with only peaks from the copper substrate being observed (Fig. 3d). Considering that the grown film contained both indium and antimony (Table III) but diffraction peaks of neither InSb nor the elements were prominent, it must be concluded that the material was amorphous.

Figure 4 shows the XRD patterns of the InSb films deposited from the baths containing different concentrations of sodium citrate. For low concentrations of sodium citrate (0.05 M to 0.15 M), the diffraction patterns (a–c) contain several peaks for In (101), In (002), In (112), In (211), and In (202) along with those of InSb. The InSb peaks became sharper and the In peaks weaker with increasing sodium citrate ion concentration in the bath. All the In peaks disappeared completely for the thin films electrodeposited using 0.2 M citrate, except for a minor In (101) peak which still remained. Thus, sharp diffraction peaks of InSb with a very low-intensity peak of In were observed for the thin films deposited using the bath containing 0.2 M citrate ions. However, when the concentration of sodium citrate was further increased beyond 0.3 M, the intensity of InSb diffraction peaks reduced, revealing that the crystallinity of the InSb thin films deteriorated at higher sodium citrate concentrations. This may be due to the deviation from stoichiometry (as seen by EDAX). The observed d values (interplanar spacings) of InSb for the samples obtained using different complexing agents are presented in Table I, while the data for films grown using different concentrations of citrate ions are presented in Table II. The values are in good agreement with standard d values for samples grown using 0.2 M sodium citrate and 0.2 M sodium tartrate. The XRD results thus show that, for the bath conditions and electrode potential used in this work, good-quality InSb films can be synthesized only using 0.2 M sodium citrate or 0.2 M sodium tartrate.

Surface Morphology and Compositional Studies

Figure 5 shows SEM images of InSb thin films electrodeposited on copper substrates from various baths with or without additional complexing agents, other than citric acid. The SEM image for the film electrodeposited without using any complexing

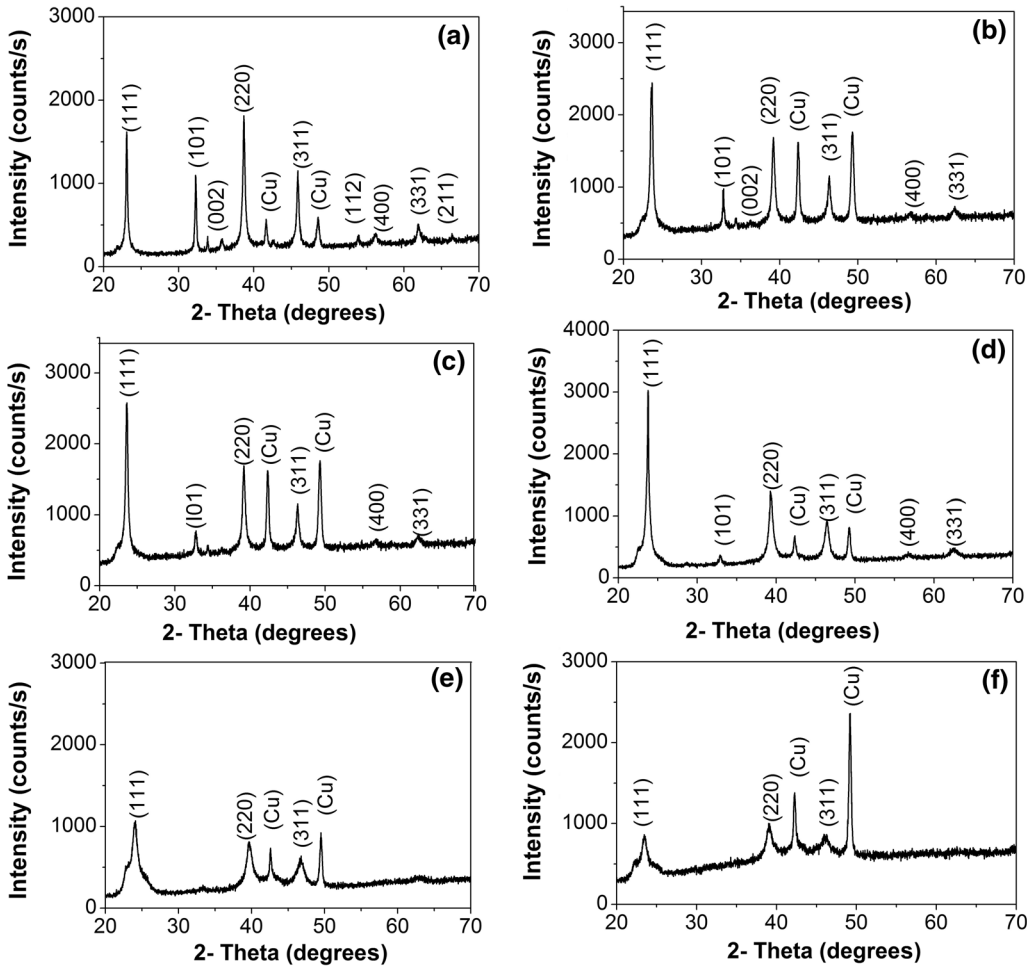

Fig. 4. XRD patterns of InSb thin films grown from baths containing 0.05 M $InCl_3$, 0.04 M $SbCl_3$, and 0.30 M citric acid with (a) 0.05 M sodium citrate, (b) 0.10 M sodium citrate, (c) 0.15 M sodium citrate, (d) 0.20 M sodium citrate, (e) 0.30 M sodium citrate, and (f) 0.40 M sodium citrate.

Table I. Comparison between observed and standard *d* values of InSb thin films grown using different complexing agents

S. no.	Standard *d* value (Å)	*hkl* plane	0.0 M sodium citrate (Å)	0.2 M sodium tartrate (Å)	0.2 M sodium citrate (Å)	0.2 M EDTA (Å)
1	3.74	(111)	3.78	3.74	3.74	–
2	2.29	(220)	2.32	2.28	2.29	–
3	1.95	(311)	1.96	1.95	1.95	–
4	1.62	(400)	1.64	1.62	1.62	–
5	1.48	(331)	–	1.48	1.48	–

agent shows cotton flower-like growth (Fig. 5a). The particles have random shapes and sizes, suggesting irregular nucleation and growth. Figure 5b shows a SEM image of the sample grown using sodium citrate, revealing denser and more compact spherical particles with size of 0.1 μm to 0.5 μm, distributed uniformly over the surface. This indicates well-controlled release of Sb^{3+} ions in the bath containing sodium citrate. When sodium tartrate was used as complexing agent, the films showed spherical submicron-sized particles, agglomerated into large bunches, as shown in Fig. 5c. The films prepared using EDTA as complexing agent showed irregular plate-like particles (Fig. 5d), formed due to large cracks on the surface of the films.

Figure 6 shows SEM images of electrodeposited InSb thin films grown on copper substrates using baths with different concentrations of citrate ions. The films synthesized using different concentrations of sodium citrate ranging from 0.05 M to

Table II. Comparison between observed and standard *d* values of InSb thin films grown using different concentrations of sodium citrate in the bath

S. no.	Standard *d* value (Å)	*hkl* plane	Concentration of sodium citrate in bath					
			0.05 M (Å)	0.1 M (Å)	0.15 M (Å)	0.20 M (Å)	0.30 M (Å)	0.40 M (Å)
1	3.74	(111)	3.77	3.75	3.75	3.74	3.75	3.78
2	2.29	(220)	2.30	2.28	2.29	2.29	2.29	2.30
3	1.95	(311)	1.98	1.94	1.95	1.95	1.94	1.96
4	1.62	(400)	1.63	–	1.62	1.62	–	–
5	1.48	(331)	1.49	1.41	1.48	1.48	1.48	–

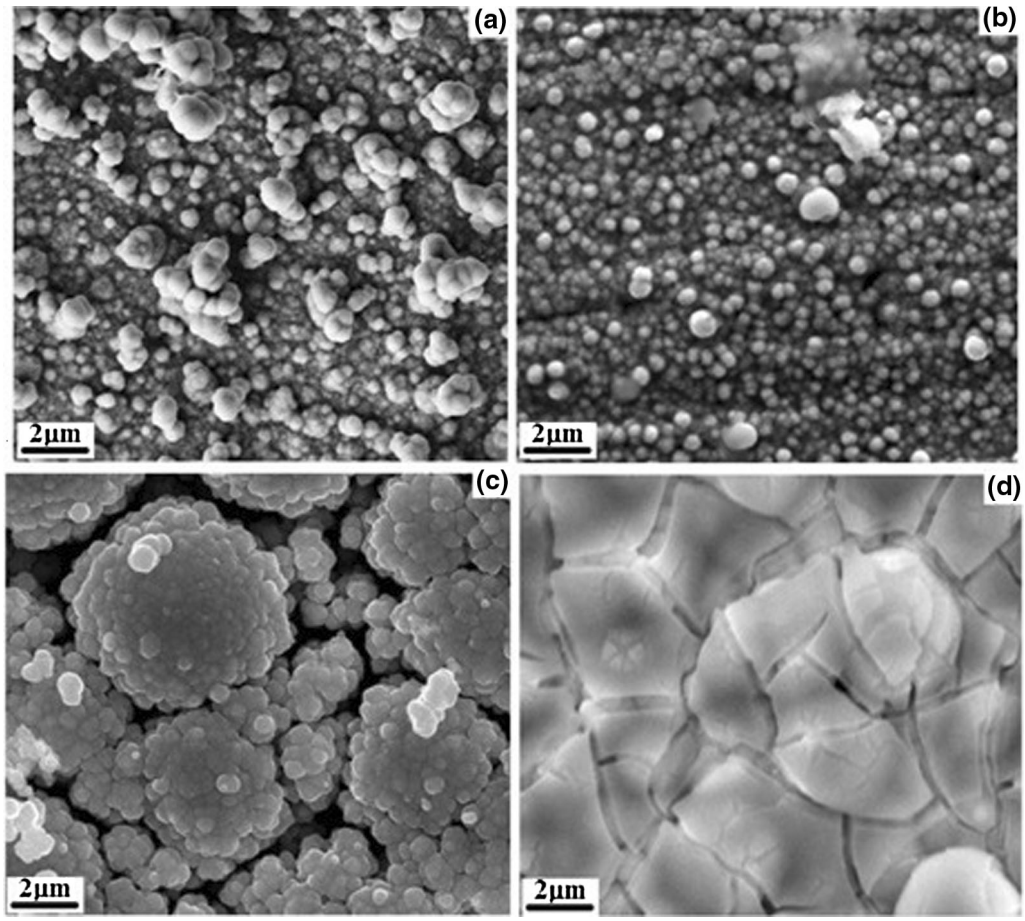

Fig. 5. SEM images of InSb thin films grown from baths containing 0.05 M $InCl_3$, 0.04 M $SbCl_3$, and 0.30 M citric acid with (a) no additional complexing agent, (b) 0.20 M sodium citrate, (c) 0.20 M sodium tartrate, and (d) 0.20 M EDTA.

0.15 M exhibited cauliflower-shaped particles or clusters. However, when the concentration of sodium citrate was increased to 0.2 M, the morphology changed to uniform growth of spherical particles with size ranging from 0.1 μm to 0.5 μm (Fig. 6d). Increasing the concentration of sodium citrate to 0.3 M did not result in any significant change in morphology, although the particle sizes became slightly larger (Fig. 6e). The films deposited from the bath containing 0.4 M sodium citrate showed fewer but much larger particles. However, several large cracks were evident on the surface of the film. Figure 7 shows the EDS mapping image along with EDAX spectrum of an InSb thin film grown using 0.2 M sodium citrate. The images confirm that the elements In and Sb were distributed fairly uniformly on the film surface. The EDAX compositions of the InSb thin films prepared using different complexing agents and different concentrations of sodium citrate are presented in Tables III and IV, respectively. From Table III, it can be seen that nonstoichiometric InSb thin films were grown

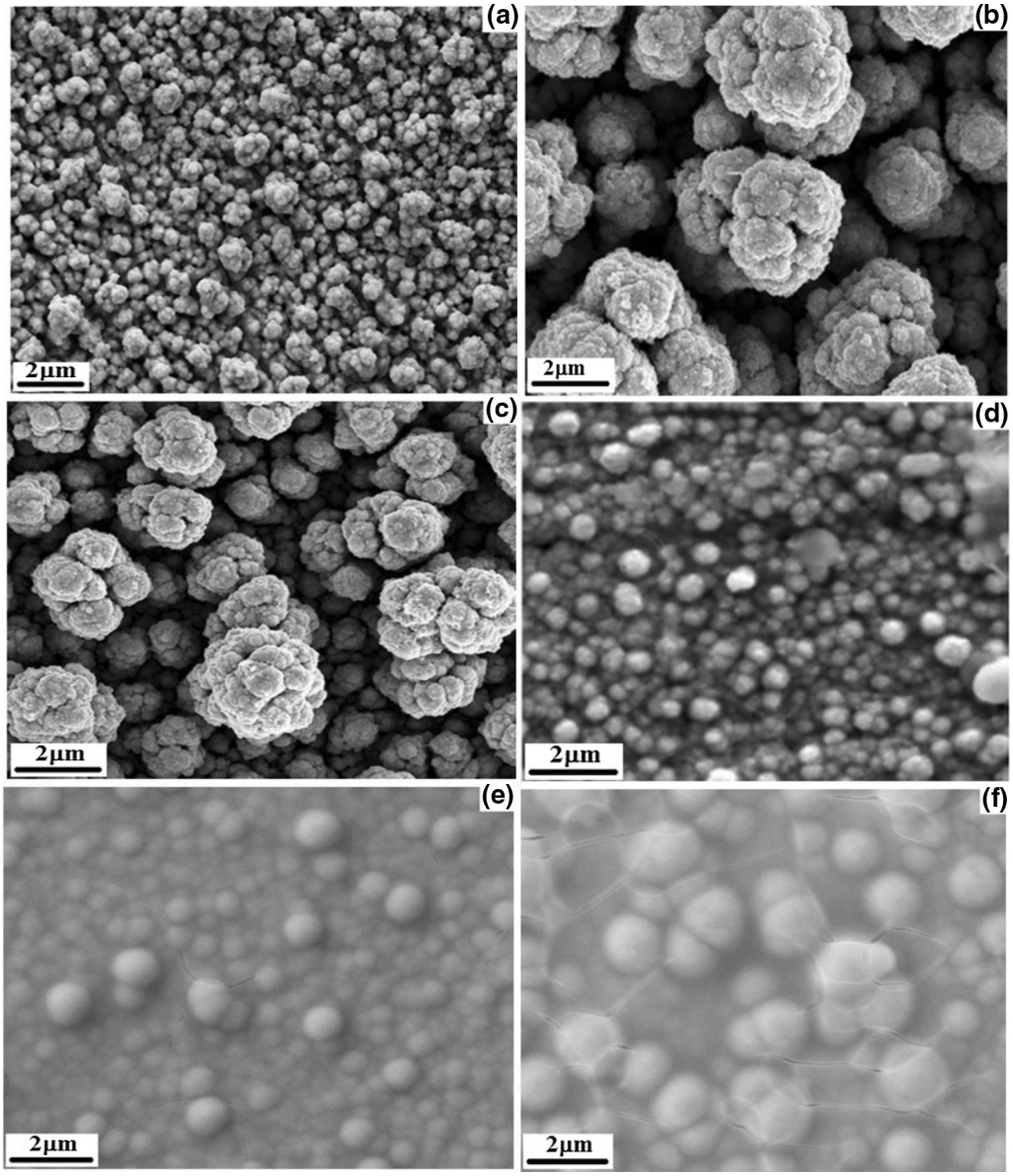

Fig. 6. SEM images of InSb thin films grown from baths containing 0.05 M $InCl_3$, 0.04 M $SbCl_3$, and 0.30 M citric acid with (a) 0.05 M sodium citrate, (b) 0.10 M sodium citrate, (c) 0.15 M sodium citrate, (d) 0.20 M sodium citrate, (e) 0.30 M sodium citrate, and (f) 0.40 M sodium citrate.

from the baths without additional complexing agent, and also when grown using EDTA as complexing agent. The elemental compositions of In and Sb in the thin films were very close to the required stoichiometry when sodium citrate and sodium tartrate were used as complexing agents. It can be seen from Table IV that the stoichiometry of the films depended on the concentration of complexing agent in the bath. The stoichiometry of the films improved as the concentration of sodium citrate ions in the bath was increased from zero, and good stoichiometric thin films were obtained for 0.2 M sodium citrate. Stoichiometric codeposition of InSb requires that the reduction potentials of both elements be the same, and addition of sodium citrate or sodium tartrate brings the potentials close to each other. The correct quantity of complexing agent is that which allows deposition of both elements at the same rate using a single electrode potential. For the present bath composition, addition of 0.2 M of the complexing agents seems to be the right amount. When the concentration of sodium citrate was increased beyond 0.3 M, the composition of the films again deviated from stoichiometry. This shows that selection of the correct concentration of complexation agent (sodium citrate) is important to achieve electrodeposited films with good crystallinity (as seen by

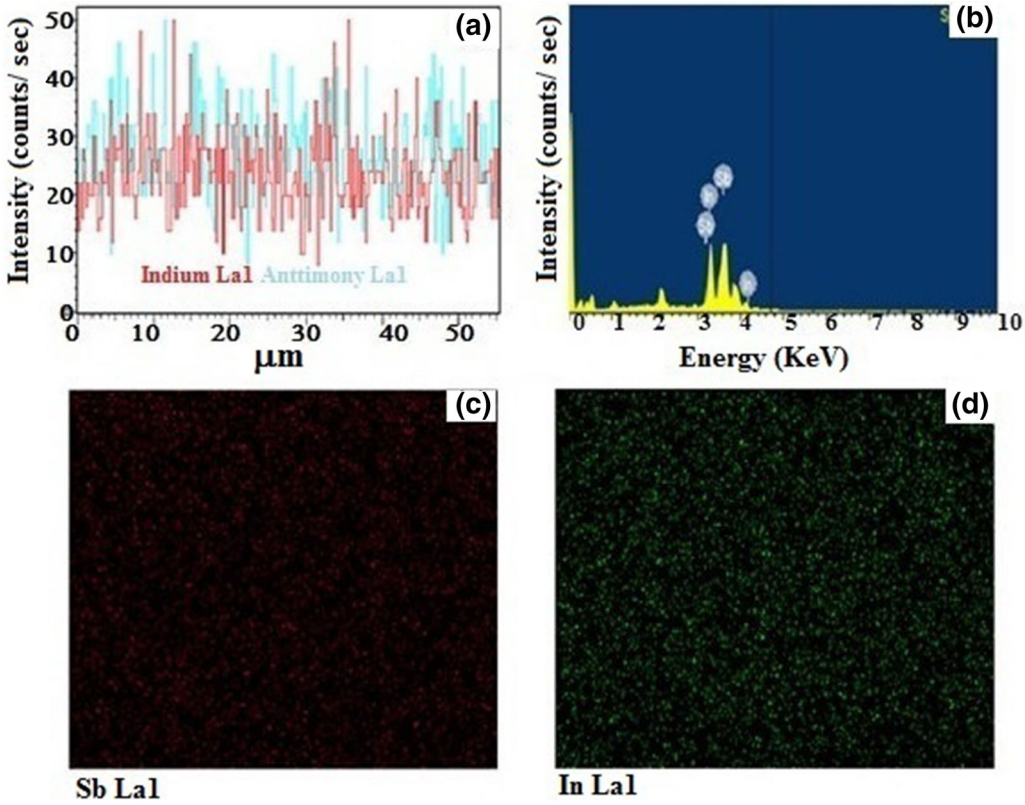

Fig. 7. EDS mapping images of an InSb thin film grown from a bath containing 0.05 M $InCl_3$, 0.04 M $SbCl_3$, 0.30 M citric acid, and 0.20 M sodium citrate, showing (a) surface intensity profile of In and Sb atoms, (b) EDAX spectrum, and elemental maps of (c) Sb and (d) In.

Table III. Elemental compositions of In and Sb in films grown using different complexing agents

S. no.	Atomic ratio in thin film (%)	0.0 M sodium citrate	0.2 M sodium tartrate	0.2 M sodium citrate	0.2 M EDTA
1	In	68.58	49.98	50.10	20.10
2	Sb	31.42	50.02	49.90	79.90

Table IV. Elemental compositions of In and Sb in films grown using different concentrations of sodium citrate

S. no.	Atomic ratio in thin film (%)	Concentration of sodium citrate in bath					
		0.05 M	0.10 M	0.15 M	0.20 M	0.30 M	0.40 M
1	In	65.73	58.76	52.26	49.98	48.98	46.74
2	Sb	34.27	41.24	47.74	50.02	51.02	53.26

XRD analysis), good morphology, and good stoichiometry (as seen by EDAX).

Raman Studies

Raman spectra of the InSb thin films grown using different complexing agents are shown in Fig. 8. Peaks corresponding to the transverse optical (TO) mode at 178 cm^{-1} and longitudinal optical (LO) mode at 189 cm^{-1} were observed for the sample grown using sodium citrate, in close agreement with TO and LO peaks reported in previous studies on InSb nanowires.[49,50] The presence of these two clearly separate peaks for the TO and LO phonon

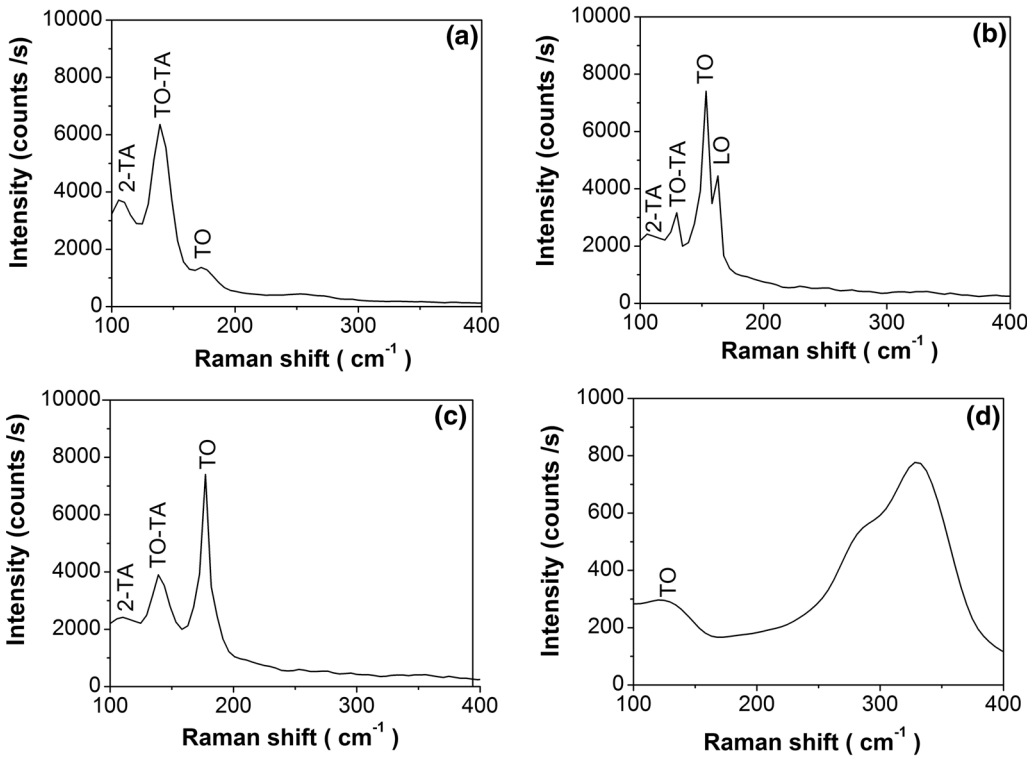

Fig. 8. Raman spectra of InSb thin films grown from baths containing 0.05 M $InCl_3$, 0.04 M $SbCl_3$, and 0.30 M citric acid with (a) no additional complexing agent, (b) 0.20 M sodium citrate, (c) 0.20 M sodium tartrate, and (d) 0.20 M EDTA.

vibrational modes indicates that good-quality InSb films were electrodeposited when using sodium citrate as complexing agent. The extra peaks (TO-TA and 2-TA) observed at about 134 cm^{-1} and 110 cm^{-1}, respectively, have been attributed to surface roughness and defects in InSb samples.[51] These extra peaks are seen for three samples (a–c) in Fig. 8. The films grown using sodium tartrate showed a single intense peak corresponding to the transverse optical (TO) mode at 178 cm^{-1}, along with additional peaks at 134 cm^{-1} and 110 cm^{-1}. Films grown from the electrolyte without additional complexing agent exhibited a minor TO peak of InSb, along with the defect/surface roughness peaks. Similarly, those grown using EDTA as complexing agent showed no peaks of InSb in the Raman spectrum, suggesting that the grown material was noncrystalline in nature.

Figure 9 shows the Raman spectra of InSb thin films obtained using different concentrations of sodium citrate. At very low sodium citrate concentrations, only TO-TA and 2TA peaks with a less intense TO peak were observed in the samples (a), suggesting growth of nonstoichiometric inhomogeneous films. With increase in the sodium citrate ion concentration, the intensity of the TO mode peak of InSb increased while that of the TO-TA and 2TA peaks decreased (b, c). When the concentration of sodium citrate in the bath was 0.2 M (d), two distinct corresponding to the transverse optical mode at 178 cm^{-1} and longitudinal optical mode at 189 cm^{-1} were seen in the Raman spectrum. These Raman results corroborate the XRD results in that the crystallinity of the films improved with increase in the sodium citrate concentration and the best-quality InSb thin films were electrodeposited using an optimum concentration (0.2 M) of sodium citrate in the bath. Further increase in the concentration of complexing agent beyond 0.3 M (e, f) led to a decrease in the intensity of the TO mode peak, indicating deterioration in film crystallinity.

Optical Studies

The IR optical transmission spectra of the InSb thin films electrodeposited using sodium citrate as complexing agent were recorded to evaluate the optical bandgap. The spectrum for one of the films grown using 0.2 M sodium citrate is shown in Fig. 10a. The energy bandgap E_g of the film was determined using the standard relation for direct optical transition, $(\alpha h\upsilon) = A(h\upsilon - E_g)^{1/2}$,[2] where A is a constant and $h\upsilon$ is the photon energy. After plotting $(\alpha h\upsilon)^2$ versus the photon energy $h\upsilon$, the value of the

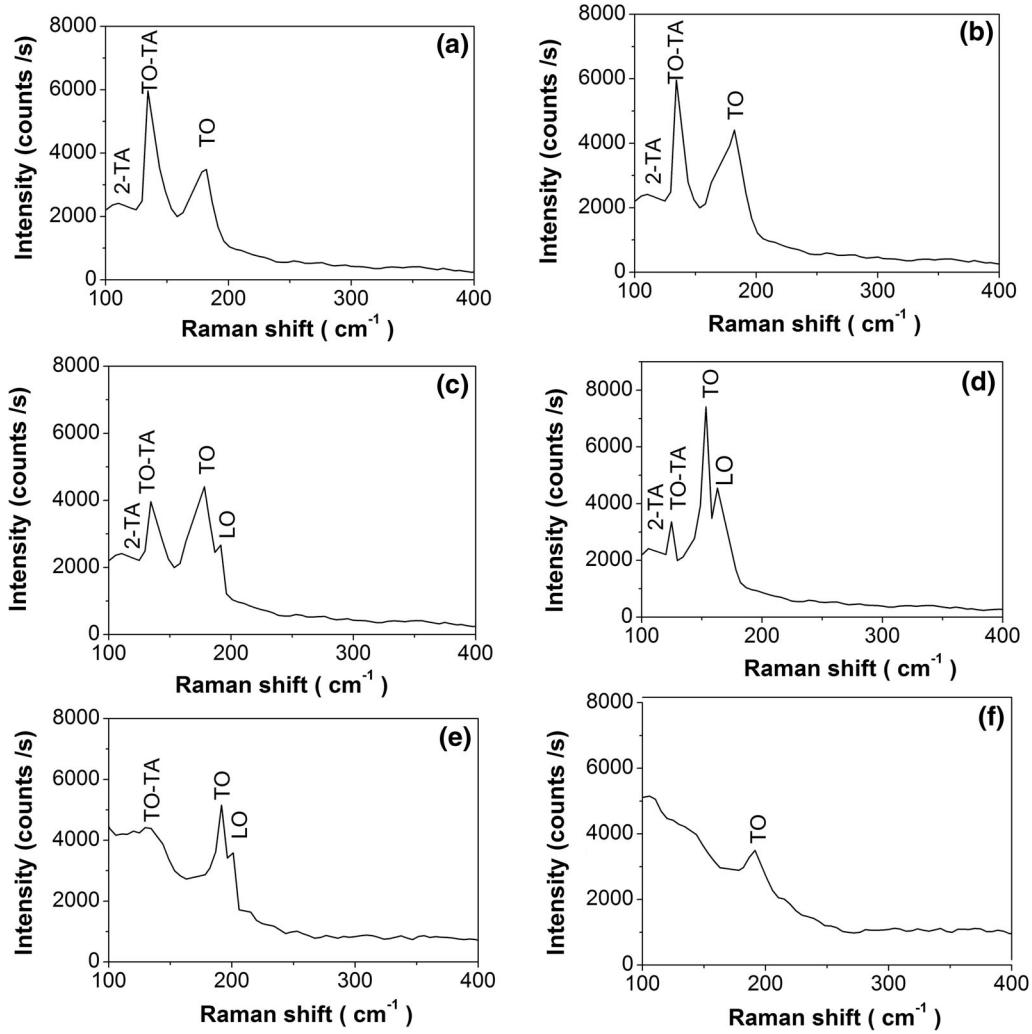

Fig. 9. Raman spectra of of InSb thin films grown from baths containing 0.05 M $InCl_3$, 0.04 M $SbCl_3$, and 0.30 M citric acid with (a) 0.05 M sodium citrate, (b) 0.10 M sodium citrate, (c) 0.15 M sodium citrate, (d) 0.20 M sodium citrate, (e) 0.30 M sodium citrate, and (f) 0.40 M sodium citrate.

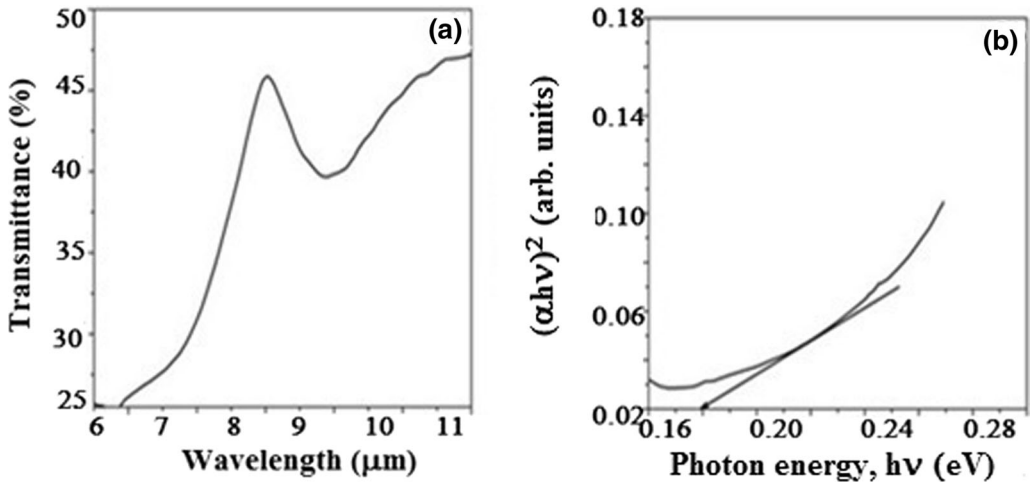

Fig. 10. (a) Transmission spectrum and (b) $(\alpha h\upsilon)^2$ versus $h\upsilon$ plot for InSb thin film grown from a bath containing 0.05 M $InCl_3$, 0.04 M $SbCl_3$, 0.30 M citric acid, and 0.2 M sodium citrate.

direct optical gap can be determined by the linear intercept with the $h\upsilon$ axis. The observed bandgap for the sample grown using 0.2 M sodium citrate is 0.18 eV, close to the reported value of 0.17 eV.[52,53]

CONCLUSIONS

InSb thin films were prepared on copper substrates by a single-step electrodeposition method from aqueous solutions using, apart from citric acid, various additives such as sodium citrate or sodium tartrate as complexing agent. The effects of the complexing agents on the structural, morphological, and compositional properties of the InSb thin film were investigated. XRD, SEM, and EDAX studies revealed that good-quality polycrystalline thin films with good stoichiometry and uniform growth could be achieved when adding 0.2 M sodium citrate or sodium tartrate to the electrolytic bath. SEM studies showed that, for low concentration of sodium citrate ions, the thin films exhibited cauliflower surface morphology, which changed to spherical particles when the concentration of citrate ions in the bath was increased to 0.2 M or beyond. The presence of TO and LO modes in the Raman spectra also indicated that the best-quality InSb thin films were electrodeposited when using the optimum concentration (0.2 M) of sodium citrate in the bath, confirming the XRD, SEM, and EDAX results.

ACKNOWLEDGEMENTS

The authors are grateful to Mr. S.D. Sharma and Mr. Shiv Kumar, IIC, IIT Roorkee, India for providing the XRD and SEM/EDAX facilities. We are also grateful to Mr. Vishnu N.R, Mahatma Gandhi University, Kerala, for the Raman facilities, and to SAIF, Punjab University, Chandigarh, for the FTIR facilities.

REFERENCES

1. X. Zhang, Y. Hao, G. Meng, and L. Zhang, *J. Electrochem. Soc.* 152, 664 (2005).
2. R.K. Mangal and Y.K. Vijay, *Bull. Mater. Sci.* 30, 117 (2007).
3. N. Kotera, T. Oi, K. Sato, J. Shigeta, N. Yamamoto, and M. Nakashima, *Thin Solid Films* 36, 483 (1976).
4. K.L. Litvinenko, L. Nikzad, J. Allam, B.N. Murdin, R.C. Pidgeon, J.J. Harris, and L.F. Cohen, *J. Supercond. Nov. Magn.* 20, 461 (2007).
5. H.A. Nilsson, P. Caroff, C. Thelander, M. Larsson, J.B. Wagner, L.E. Wernersson, L. Samuelson, and H.Q. Xu, *Nano Lett.* 9, 315 (2009).
6. I. Kimukin, N. Biyikli, T. Kartaloglu, O. Ayt, and E. Ozbay, *IEEE J. Sel. Top. Quant. Electron.* 10, 766 (2004).
7. A. Rogalski, *Infrared Phys. Technol.* 43, 187 (2002).
8. T. Ashley, A.B. Dean, C.T. Elliott, R. Jefferies, F. Khaleque, and T.J. Phillips, *Int. Electron Dev. Meet.* 751 (1997).
9. B.M. Borg and L.E. Wernerson, *Nanotechnology*, 24, 1 (2013).
10. J.A. Alamodel, *Nature* 479, 317 (2011).
11. J. Heremans, D.L. Partin, and C.M. Thrush, *Semicond. Sci. Technol.* 8, 424 (1993).
12. S.A. Solin, T. Thio, D.R. Hines, and J.J. Heremans, *Science* 289, 15 (2000).
13. M. Ohshita, *Sens. Actuators A* 40, 131 (1994).
14. M.K. Carpenter and M.W. Verbrugge, *J. Mater. Res.* 9, 2584 (1994).
15. T. Ashley, A.B. Dean, C.T. Elliott, G.J. Pryce, A.D. Johnson, and H. Willis, *Appl. Phys. Lett.* 66, 481 (1995).
16. J.E. Cornett and O. Rabin, *Appl. Phys. Lett.* 98, 182104 (2011).
17. N. Mingo, *Appl. Phys. Lett.* 84, 2652 (2004).
18. T. Miyazaaki, M. Kunugi, Y. Kitamure, and S. Adachi, *Thin Solid Films* 287, 51 (1996).
19. D. Ercolani, F. Rossi, A. Li, S. Roddaro, V. Grillo, G. Salviati, F. Beltram, and L. Sorba, *Nanotechnology*, 20, 505605 (2009).
20. A.T. Vogel, J. de Boor, J. Wittemann, S.L. Mensah, P. Werner, and V. Schmidt, *Cryst. Growth Des.* 11, 1896 (2011).
21. T.R. Yang, Y. Cheng, J.B. Wang, and Z.C. Feng, *Thin Solid Films* 498, 158 (2006).
22. D.L. Partin, L. Green, and J. Heremans, *J. Electron. Mater.* 23, 75 (1994).
23. V. Senthilkumar, M. Thamilselvan, P.K. Nazeer, S.K. Narayandass, D. Mangalaraj, B. Karunagaran, K. Kim, and J. Yi, *Vacuum*, 79, 163 (2005).
24. R.N. Bhattacharya, J.F. Hiltner, W. Batchelor, M.A. Contreras, R.N. Noufi, and J.R. Sites, *Thin Solid Films*, 361 (2000).
25. K. Singh and R. Tanveer, *Sol. Energy Mater. Sol. Cells* 36, 409 (1995).
26. Z. Zainal, N. Saravanan, and H.L. Mien, *Mater. Electron.* 16, 111 (2005).
27. F. Zhou, A.L. Moore, M.T. Pettes, Y. Lee, J.H. Seol, Q.L. Ye, L. Rabenberg, and L. Shi, *J. Phys. D Appl. Phys.* 43, 025406 (2010).
28. U. Philipose, G. Sapkota, J. Salfi, and H.E. Ruda, *Semicond. Sci. Technol.* 25, 075004 (2010).
29. Encyclopedia of electrochemistry of the elements, vol. VI 1973–ISBN 0824725069.
30. Z. Zainal, S. Nagalingam, and T.M. Hua, *Mater. Electron.* 16, 281 (2005).
31. S.C. Liufu, L.D. Chen, Q. Yao, and F.Q. Huang, *J. Phys. Chem.* 11, 12085 (2008).
32. J. Machesney, J. Haigh, I.M. Dharmadasa, and D.J. Mowthorpe, *Opt. Mater.* 6, 63 (1996).
33. T. Fulop, C. Bekele, U. Landau, J. Angus, and K. Kash, *Thin Solid Films* 449, 1 (2004).
34. M.I. Khan, X. Wang, X. Jing, K.N. Bozhilov, and C.S. Ozkan, *J. Nanosci. Nanotechnol.* 8, 1 (2008).
35. M.I. Khan, X. Wang, X. Jing, K.N. Bozhilov, and C.S. Ozkan, J. Nanomater, https://doi.org/10.1155/2008/698759.
36. K.E. Hnida, L. Akinsinde, J. Gooth, K. Nielsch, R.P. Socha, A. Łaszcz, A. Czerwinski, and G.D. Sulka, *J. Mater. Chem. C* 4, 1345 (2016).
37. A. Singh, Z. Algarni, and U. Philiposez, *ECS J. Solid State Sci. Technol.*, 6, 39 (2017).
38. S.R. Das, C.J. Delker, D. Zakharov, Y.P. Chen, T.D. Sands, and D.B. Janes, *Appl. Phys. Lett.* 98, 243504 (2011).
39. Y.T. Hsieh, Y.C. Chen, and I.W. Sun, *Chem. Electro. Chem.*, 3, 638 (2016).
40. M.H. Yang, M.C. Yang, and I. Wen, *J. Electrochem. Soc.* 150, 544 (2003).
41. J. Singh and R. Poolla, *Mater. Electron.* 28, 3716 (2017).
42. F. Chraibi, M. Fahoume, A. Ennaoui, and J.L. Delplancke, *Phys. Stat. Sol.* 186, 373 (2001).
43. Encyclopedia of electrochemistry of the elements, vol. VI 1973 –ISBN 0824725069.
44. D. Grujicic and B. Pesic, *Electrochem. Acta* 47, 2901 (2002).
45. L. Zhou, Y. Dai, H. Zhang, Y. Jia, J. Zhang, and C. Li, *Bull. Korean Chem. Soc.* 33, 1541 (2012).
46. J. Liu and T. Zhang, *Appl. Surf. Sci.* 126, 231 (1998).
47. S.V. Stariy, A.V. Sukach, V.V. Tetyorkin, V.O. Yukhymchuk, and T.R. Stara, *Quantum Electron. Optoelectron.*, 20, 105 (2017).
48. C.J. Koswaththage, T. Okada, T. Noguchi, S. Taniguchi, and S. Yoshitome, *AIP Adv.* 6, 115303 (2016).
49. A. Pinczuk and E. Burstein, *Phys. Rev. Lett.* 21, 1073 (1968).

50. W. Kiefer, W. Richter, and M. Cardona, *Phys. Rev. B* 12, 2346 (1975).
51. N. Wada, H. Takayama, and S. Morohashi, APS March meeting 55, Portland, Oregon, March 15–19, 2010, Abstract No. L9.013.
52. S. Singh, K. Lal, A.K. Srivastava, K.N. Sood, and R. Kishore, *Indian J. Eng. Mater. Sci.* 14, 55 (2007).
53. R.K. Mangal, Y.K. Vijay, D.K. Avasthi, and B.R. Shekhar, *Indian J. Eng. Mater. Sci.* 14, 253 (2007).